Effect of boson on-site repulsion on the superfluidity in the boson-fermion-Hubbard model

A. S. Sajna and R. Micnas

Solid State Theory Division, Faculty of Physics, Adam Mickiewicz University, ulica Umultowska 85, 61-614 Poznań, Poland

We analyze the finite-temperature phase diagram of the boson-fermion-Hubbard model with Feshbach converting interaction, using the coherent-state path-integral method. We show that depending on the position of the bosonic band, this type of interaction, even if weak, can drive the system into the resonant superfluid phase in the strong bosonic interaction limit. It turns out that this phase can exist for an arbitrary number of fermions (i.e., fermionic concentration between 0 and 2), but with the bosonic particle number very close to an integer value. We point out that the standard time-of-flight method in optical lattice experiments can be an adequate technique to confirm the existence of this resonant phase. Moreover, in the nonresonant regime, the enhancement of the critical temperature of the superfluid phase due to Feshbach interaction is also observed. We account for this interesting phenomena for a hole- or particlelike pairing mechanism depending on the system density and mutual location of the fermionic and bosonic bands.

I. INTRODUCTION

The boson-fermion-Hubbard model (BFHM) with a resonant pairing mechanism has a very long history in the context of high-temperature superconductivity (see, e.g., [1–15], and references therein). Recently, the interest in this model has been extended to the ultracold-atomic systems because they are a versatile tool for simulating many-body physics [16–18], and the BFHM can be studied by using Feshbach resonance experiments in which the BCS-BEC crossover is realized [18–21].

The impact of strong bosonic interaction on the superfluid (SF) phase in the lattice bosons system has been widely investigated in the literature in terms of the Bose-Hubbard model (BHM) (e.g., see [22], and reference therein). However, the superfluidity in the regime of strong bosonic repulsion in which Feshbach interaction is included is much less understood. So far only the hard-core limit [2,3,23–25] and some qualitative studies have been performed [26]. Therefore, in this paper, quantitative investigation of the nonzero-temperature BFHM phase diagram with finite bosonic repulsion interaction is carried out, which is relevant for working out realistic experimental conditions. The effective field theory description of the BFHM is constructed by using the coherent-state path-integral formalism. This analytical method seems to be a good starting point for analysis of the BFHM because it provides a reasonable description of the standard Fermi-Hubbard model at weak interparticle interaction (i.e., in the BCS regime) [27] and it also gives a correct description of the BHM [28]. In this paper, we show that besides the standard superfluid phase which is governed by the pure bosonic correlation mechanism present in the BHM, there also appears a resonant superfluid (RSF) phase due to the Feshbach resonance phenomena. Moreover, we explain that the standard superfluid phase (not RSF) is enhanced by the hole- or particle-pairing mechanism of fermions. The results allow us to discuss an experimental proposal for the possible investigation of a RSF phase in the BFHM.

In the following sections, we first describe the model and apply the coherent-state path-integral method (Sec. II). Then, in Sec. III, we use this method in the analysis of the finite-temperature phase diagram of the BFHM and its thermodynamic quantities. At the end of Sec. III, we also discuss experimental setups that could be used to prove some results of our theory. Finally, in Sec. IV, we give a summary of our work. Moreover, the Appendix contains additional investigations of the BFHM model within the operator approach.

II. MODEL AND METHOD

A. Model

We consider the boson-fermion-Hubbard model (BFHM) with converting interaction energy I, whose Hamiltonian is given by [15,23]

$$H = -\sum_{ij\sigma}(t_{ij} + \mu\delta_{ij})c^\dagger_{i\sigma}c_{j\sigma} - V\sum_i c^\dagger_{i\uparrow}c^\dagger_{i\downarrow}c_{i\downarrow}c_{i\uparrow}$$
$$- \sum_{ij}(J_{ij} + \mu^*\delta_{ij})b^\dagger_i b_j + \frac{U}{2}\sum_i b^\dagger_i b^\dagger_i b_i b_i$$
$$+ I\sum_i [c^\dagger_{i\uparrow}c^\dagger_{i\downarrow}b_i + b^\dagger_i c_{i\downarrow}c_{i\uparrow}], \qquad (1)$$

where μ is the chemical potential, $\mu^* = 2\mu - 2\Delta_B$, and σ is a spin-$\frac{1}{2}$ index ($\sigma \in \{\uparrow,\downarrow\}$). $c_{i\sigma}$ ($c^\dagger_{i\sigma}$) is the fermionic annihilation (creation) operator at site i with spin σ, and b_i ($b^\dagger_i$) is the bosonic annihilation (creation) operator at site i. The hopping energies for fermions and bosons are t_{ij} and J_{ij}, respectively. Throughout this work, we restrict hopping parameters to the nearest-neighbor sites. Moreover, U denotes the on-site interaction energy of bosons, which will be treated exactly during calculations, and V is the fermionic on-site interaction strength. The bottom of the bosonic band is shifted by the $2\Delta_B$ parameter, which could be tuned in ultracold-atom experiments with the Feshbach resonance [18,19,21,29].

Interestingly, if we assume $I = 0$ and independent chemical potentials, the BFHM Hamiltonian [Eq. (1)] describes two independent models, i.e., the fermionic and bosonic Hubbard models. However, in the presence of finite resonant interaction ($I \neq 0$), there is only one phase transition from the superfluid phase, which we will show shortly.

Further, in the case of $U = V = 0$, the model described by the Hamiltonian in Eq. (1) was previously investigated in the continuum and lattice systems [15,20,23,30–32]. Moreover, when $U \to \infty$, the hard-core bosonic limit is obtained for which bosonic operators satisfy the Pauli spin-1/2 commutations relations [2,3,9,15,23].

In the coherent-state path-integral representation, the partition function of BFHM reads

$$Z = \int \mathcal{D}[\bar{c},c,\bar{b},b]e^{-\frac{1}{\hbar}S[\bar{c},c,\bar{b},b]}, \qquad (2)$$

where the action is given by

$$S[\bar{c},c,\bar{b},b] = S_0^F[\bar{c},c] + S_0^B[\bar{b},b] + S_0^{\text{FB}}[\bar{b},b,\bar{c},c] + S_1^B[\bar{b},b]. \qquad (3)$$

The denotation is related to the perturbed and unperturbed parts of the action, which we exploit further, i.e., the unperturbed parts are

$$S_0^F[\bar{c},c] = \int_0^{\hbar\beta} d\tau \left\{ \sum_{i\sigma} \bar{c}_{i\sigma}(\tau)\hbar\frac{\partial}{\partial\tau}c_{i\sigma}(\tau) \right.$$
$$+ \sum_{ij\sigma}(-t_{ij} - \mu\delta_{ij})\bar{c}_{i\sigma}(\tau)c_{j\sigma}(\tau)$$
$$\left. - V\sum_i \bar{c}_{i\uparrow}(\tau)\bar{c}_{i\downarrow}(\tau)c_{i\downarrow}(\tau)c_{i\uparrow}(\tau) \right\}, \qquad (4)$$

$$S_0^B[\bar{b},b] = \sum_i \int_0^{\hbar\beta} d\tau \left\{ \bar{b}_i(\tau)\hbar\frac{\partial}{\partial\tau}b_i(\tau) - \mu^*\bar{b}_i(\tau)b_i(\tau) \right.$$
$$\left. + \frac{U}{2}\bar{b}_i(\tau)\bar{b}_i(\tau)b_i(\tau)b_i(\tau) \right\}, \qquad (5)$$

$$S_0^{\text{FB}}[\bar{b},b,\bar{c},c] = I\sum_i \int_0^{\hbar\beta} d\tau[\bar{c}_{i\uparrow}(\tau)\bar{c}_{i\downarrow}(\tau)b_i(\tau) + \text{c.c.}], \qquad (6)$$

and the part of the action which we will treat approximately is

$$S_1^B[\bar{b},b] = -\sum_{ij} \int_0^{\hbar\beta} d\tau J_{ij}\bar{b}_i(\tau)b_j(\tau). \qquad (7)$$

The fields $c_{i\sigma}(\tau)$, $\bar{c}_{i\sigma}(\tau)$ are Grassmann variables, the $b_i(\tau)$, $\bar{b}_i(\tau)$ are complex variables, $\hbar$ is the reduced Planck constant, and $\beta = 1/k_B T$, where k_B and T denote the Boltzmann constant and temperature, respectively. Throughout this work, we denote the complex conjugation of the arbitrary x variable by $\bar{x}$.

B. Effective action

We are interested in the influence of the fermionic degrees of freedom on the bosonic part in the BFHM model within the $J \ll U$ limit.

In the first step, the term describing the interaction between fermionic particles is decoupled by the Hubbard-Stratonovich (HS) transformation in the pairing channel, which introduces the $\Delta_i(\tau)$, $\bar{\Delta}_i(\tau)$ fields [27]. Then, $S_0^F[\bar{c},c,] \to \tilde{S}_0^F[\bar{c},c,\bar{\Delta},\Delta]$, where

$$\tilde{S}_0^F[\bar{c},c,\bar{\Delta},\Delta]$$
$$= \int_0^{\hbar\beta} d\tau \left\{ \sum_{i\sigma} \bar{c}_{i\sigma}(\tau)\hbar\frac{\partial}{\partial\tau}c_{i\sigma}(\tau) \right.$$
$$- \sum_i \bar{c}_{i\uparrow}(\tau)\bar{c}_{i\downarrow}(\tau)\Delta_i(\tau) - \sum_i \bar{\Delta}_i(\tau)c_{i\downarrow}(\tau)c_{i\uparrow}(\tau)$$
$$\left. + \sum_{ij\sigma}(-t_{ij} - \mu\delta_{ij})\bar{c}_{i\sigma}(\tau)c_{j\sigma}(\tau) + \frac{1}{V}\sum_i |\Delta_i(\tau)|^2 \right\}, \qquad (8)$$

and for which the HS measure $\mathcal{D}[\bar{\Delta},\Delta]$ contains the determinant $\det[V^{-1}]$. Then, in the $J \ll U$ limit, we decouple the term in the action from Eq. (7) which is proportional to J. It is performed by introducing the HS transformation,

$$\sum_{ij} \int_0^{\hbar\beta} d\tau J_{ij}\bar{b}_i(\tau)b_j(\tau) \to -\sum_{ij} \int_0^{\hbar\beta} d\tau J_{ij}^{-1}\bar{\psi}_i(\tau)\psi_j(\tau)$$
$$+ \sum_i \int_0^{\hbar\beta} d\tau \bar{\psi}_i(\tau)b_i(\tau) + \sum_i \int_0^{\hbar\beta} d\tau \bar{b}_i(\tau)\psi_i(\tau). \qquad (9)$$

Going further, integrating out of the bosonic fields $\bar{b}_i(\tau)$, $b_i(\tau)$ is desirable. Before we do that, we have to apply some approximation of these fields since, in the present form, the action considered above is nonintegrable in $\bar{b}_i(\tau)$, $b_i(\tau)$ because of the interaction term proportional to U. Therefore, we rewrite the partition function from Eq. (2) in the following form:

$$Z = Z_0^B \det[\mathbf{J}^{-1}] \int \mathcal{D}[\bar{c},c,\bar{\psi},\psi,\bar{\Delta},\Delta]$$
$$\times e^{-\frac{1}{\hbar}\sum_{ij}\int_0^{\hbar\beta} d\tau J_{ij}^{-1}\bar{\psi}_i(\tau)\psi_j(\tau) - \frac{1}{\hbar}\tilde{S}_0^F[\bar{c},c,\bar{\Delta},\Delta]}$$
$$\times \left\langle e^{-\frac{1}{\hbar}\sum_i \int_0^{\hbar\beta} d\tau\{[-\bar{\psi}_i(\tau) + I\bar{c}_{i\uparrow}(\tau)\bar{c}_{i\downarrow}(\tau)]b_i(\tau) + \text{c.c.}\}} \right\rangle_0^B, \qquad (10)$$

where $\mathbf{J}$ is the hopping matrix J_{ij} which results from the HS transformation in Eq. (9), and the statistical average $\langle\cdot\rangle_0^B$ is defined as $(Z_0^B)^{-1}\int \mathcal{D}[\bar{b},b]\ldots e^{-S_0^B[\bar{b},b]/\hbar}$ with

$$Z_0^B = \int \mathcal{D}[\bar{b},b]e^{-S_0^B[\bar{b},b]/\hbar}. \qquad (11)$$

Because the $\psi_i(\tau)$, $\bar{\psi}_i(\tau)$ fields have quadratic form with linear terms, we can make the shift $\psi_i(\tau) \to \psi_i(\tau) + Ic_{i\downarrow}(\tau)c_{i\uparrow}(\tau)$ and $\bar{\psi}_i(\tau) \to \bar{\psi}_i(\tau) + I\bar{c}_{i\uparrow}(\tau)\bar{c}_{i\downarrow}(\tau)$ and obtain

$$Z = Z_0^B \det[\mathbf{J}^{-1}] \int \mathcal{D}[\bar{c},c,\bar{\psi},\psi,\bar{\Delta},\Delta]$$
$$\times e^{-\frac{1}{\hbar}\sum_{ij}\int_0^{\hbar\beta} d\tau J_{ij}^{-1}[\bar{\psi}_i(\tau) + I\bar{c}_{i\uparrow}(\tau)\bar{c}_{i\downarrow}(\tau)][\psi_j(\tau) + Ic_{j\downarrow}(\tau)c_{j\uparrow}(\tau)]}$$
$$\times e^{-\frac{1}{\hbar}\tilde{S}_0^F[\bar{c},c,\bar{\Delta},\Delta] - \frac{1}{\hbar}W_1[\bar{\psi},\psi]}, \qquad (12)$$

where we define

$$W_1[\bar{\psi},\psi] = -\hbar\ln\left\langle e^{-\frac{1}{\hbar}\sum_i \int_0^{\hbar\beta} d\tau[-\bar{\psi}_i(\tau)b_i(\tau) + \text{c.c.}]} \right\rangle_0^B. \qquad (13)$$

Within the strong-coupling approach ($J \ll U$), it is convenient to expand $W_1[\bar{\psi},\psi]$ in terms of the $\psi_i(\tau)$, $\bar{\psi}_i(\tau)$ fields,

namely,

$$
\begin{aligned}
W_1[\bar{\psi},\psi] = \sum_{p=1}^{\infty} \frac{(-1)^p}{(p!)^2} \int_0^{\hbar\beta} d\tau_1 \dots d\tau_p d\tau'_1 \dots d\tau'_p \\
\times \sum_i G_i^{p,c}(\tau'_1,\dots,\tau'_p,\tau_1,\dots,\tau_p) \\
\times \bar{\psi}_i(\tau'_1)\dots\bar{\psi}_i(\tau'_p)\psi_i(\tau_1)\dots\psi_i(\tau_p), \quad (14)
\end{aligned}
$$

where $G_i^{p,c}(\tau'_1,\dots,\tau'_p,\tau_1,\dots,\tau_p)$ are connected local Green functions,

$$
\begin{aligned}
& G_i^{p,c}(\tau'_1,\dots,\tau'_p,\tau_1,\dots,\tau_p) \\
& = \frac{(-1)^p \delta^{(2p)} W_1[\bar{\psi},\psi]}{\delta\bar{\psi}_i(\tau'_1)\dots\delta\bar{\psi}_i(\tau'_p)\delta\psi_i(\tau_1)\dots\delta\psi_i(\tau_p)}\bigg|_{\bar{\psi}=\psi=0}. \quad (15)
\end{aligned}
$$

Then, truncating $W_1[\bar{\psi},\psi]$ to quartic order and inserting the results into Eq. (12), one gets the following effective action:

$$
\begin{aligned}
& S^{\text{eff}}[\bar{c},c,\bar{\psi},\psi,\bar{\Delta},\Delta] \\
& = \tilde{S}_0^B[\bar{\psi},\psi] + \sum_{ij} \int_0^{\hbar\beta} d\tau[\bar{\psi}_i(\tau) + I\bar{c}_{i\uparrow}(\tau)\bar{c}_{i\downarrow}(\tau)] \\
& \times J_{ij}^{-1}[\psi_j(\tau) + Ic_{j\downarrow}(\tau)c_{j\uparrow}(\tau)] + \tilde{S}_0^F[\bar{c},c,\bar{\Delta},\Delta] \\
& - \frac{1}{4}\sum_i \int_0^{\hbar\beta} d\tau d\tau' d\tau'' d\tau''' G_i^{2,c}(\tau,\tau',\tau'',\tau''') \\
& \times \bar{\psi}_i(\tau''')\bar{\psi}_i(\tau'')\psi_i(\tau')\psi_i(\tau), \quad (16)
\end{aligned}
$$

with

$$
\tilde{S}_0^B[\bar{\psi},\psi] = \sum_i \int_0^{\hbar\beta} d\tau d\tau' G_i^{1,c}(\tau,\tau')\bar{\psi}_i(\tau')\psi_i(\tau). \quad (17)
$$

It is interesting to point out here that the pair-hopping term naturally emerges in the effective action from Eq. (16), i.e., the term $I^2 \sum_{ij} \int_0^{\hbar\beta} d\tau J_{ij}^{-1} \bar{c}_{i\uparrow}(\tau)\bar{c}_{i\downarrow}(\tau)c_{j\downarrow}(\tau)c_{j\uparrow}(\tau)$, and is induced by the resonant interaction I.

Further, we perform the second HS transformation in terms of J_{ij}^{-1}, i.e.,

$$
\begin{aligned}
& - \sum_{ij} \int_0^{\hbar\beta} d\tau[\bar{\psi}_i(\tau) + I\bar{c}_{i\uparrow}(\tau)\bar{c}_{i\downarrow}(\tau)] \\
& \times J_{ij}^{-1}[\psi_j(\tau) + Ic_{j\downarrow}(\tau)c_{j\uparrow}(\tau)] \\
& \rightarrow \sum_{ij} \int_0^{\hbar\beta} d\tau J_{ij}\bar{\phi}_i(\tau)\phi_j(\tau) \\
& - \left\{ \sum_i \int_0^{\hbar\beta} d\tau \bar{\phi}_i(\tau)[\psi_i(\tau) + Ic_{i\downarrow}(\tau)c_{i\uparrow}(\tau)] + \text{c.c.} \right\}, \\
& \hspace{10cm} (18)
\end{aligned}
$$

where the new HS fields are $\phi_i(\tau)$, $\bar{\phi}_i(\tau)$. In comparison to the fields from the first HS [Eq. (9)], the $\phi_i(\tau)$, $\bar{\phi}_i(\tau)$ fields have the same generating functional as the original $b_i(\tau)$, $\bar{b}_i(\tau)$ fields. Therefore, using the $\phi_i(\tau)$, $\bar{\phi}_i(\tau)$ fields is more suitable in the physical analysis because their correlation functions have the same interpretation as the correlation functions for the original $b_i(\tau)$, $\bar{b}_i(\tau)$ fields. To clarify this, in the Appendix, we add the proof that both fields have the same generating functional. Moreover, beyond this useful fact about $\phi_i(\tau)$, $\bar{\phi}_i(\tau)$, it is worth mentioning here that these fields, in the limit of the BHM (when $I = 0$), yield properly normalized density of states in the BHM superfluid phase [28] (properties of the SF spectrum in the full BFHM need further study).

After applying the second HS [Eq. (18)] to Eq. (16), the corresponding effective action is

$$
\begin{aligned}
& S^{\text{eff}}[\bar{c},c,\bar{\phi},\phi,\bar{\Delta},\Delta] \\
& = - \sum_{ij} \int_0^{\hbar\beta} d\tau J_{ij}\bar{\phi}_i(\tau)\phi_j(\tau) \\
& + \left\{ I \sum_i \int_0^{\hbar\beta} d\tau \bar{\phi}_i(\tau)c_{i\downarrow}(\tau)c_{i\uparrow}(\tau) + \text{c.c.} \right\} \\
& + \tilde{S}_0^F[\bar{c},c,\bar{\Delta},\Delta] + W_2[\bar{\phi},\phi], \quad (19)
\end{aligned}
$$

with denotation

$$
W_2[\bar{\phi},\phi] = -\hbar \ln \left\langle e^{-\frac{1}{\hbar}\sum_i \int_0^{\hbar\beta} d\tau[\bar{\phi}_i(\tau)\psi_i(\tau)+\text{c.c.}]+\frac{1}{4}\sum_i \int_0^{\hbar\beta} d\tau d\tau' d\tau'' d\tau''' G_i^{2,c}(\tau,\tau',\tau'',\tau''')\bar{\psi}_i(\tau''')\bar{\psi}_i(\tau'')\psi_i(\tau')\psi_i(\tau)} \right\rangle_0^{B,\text{eff}}, \quad (20)
$$

and where the statistical average $\langle\cdot\rangle_0^{B,\text{eff}}$ is defined as $(\tilde{Z}_0^B)^{-1} \int \mathcal{D}[\bar{\psi},\psi] \dots e^{-\tilde{S}_0^B/\hbar}$ with $\tilde{Z}_0^B = \int \mathcal{D}[\bar{\psi},\psi]e^{-\tilde{S}_0^B/\hbar}$. And, once again, by truncating $W_2[\bar{\phi},\phi]$ to the quartic order and retaining only the terms which are not "anomalous" [28,33–35], we obtained the final form of statistical sum $\tilde{Z}^{\text{eff}}$ with effective action $\tilde{S}^{\text{eff}}$ (in which the fermionic degrees of freedom were integrated out), i.e.,

$$
\tilde{Z}^{\text{eff}} = \int \mathcal{D}[\bar{\phi},\phi,\bar{\Delta},\Delta]e^{-\frac{1}{\hbar}\tilde{S}^{\text{eff}}[\bar{\phi},\phi,\bar{\Delta},\Delta]}, \quad (21)
$$

$$
\begin{aligned}
\tilde{S}^{\text{eff}}[\bar{\phi},\phi,\bar{\Delta},\Delta] = & -\text{Tr}\ln\left[-G_F^{-1}(i,j,\tau)\right] + \frac{1}{V}\sum_i |\Delta_i(\tau)|^2 - \sum_{ij}\int_0^{\hbar\beta} d\tau J_{ij}\bar{\phi}_i(\tau)\phi_j(\tau) \\
& - \sum_i \int_0^{\hbar\beta} d\tau d\tau'\left[G_i^{1,c}(\tau,\tau')\right]^{-1}\bar{\phi}_i(\tau')\phi_i(\tau) \\
& + \frac{1}{4}\sum_i \int_0^{\hbar\beta} d\tau d\tau' d\tau'' d\tau''' \Gamma_i^{2,c}(\tau,\tau',\tau'',\tau''')\bar{\phi}_i(\tau''')\bar{\phi}_i(\tau'')\phi_i(\tau')\phi_i(\tau), \quad (22)
\end{aligned}
$$

where we introduced the matrix fermionic Green function,

$$
G_F^{-1}(i, j, \tau) = \begin{bmatrix} \left(-\hbar\frac{\partial}{\partial\tau} + \mu\right)\delta_{ij} + t_{ij} & \Delta_i(\tau) - I\phi_i(\tau) \\ \bar{\Delta}_i(\tau) - I\bar{\phi}_i(\tau) & \left(-\hbar\frac{\partial}{\partial\tau} - \mu\right)\delta_{ij} - t_{ij} \end{bmatrix}, \tag{23}
$$

and effective interaction between bosons,

$$
\Gamma_i^{2,c}(\tau, \tau', \tau'', \tau''') = \frac{\delta^{(4)}W_2[\bar{\phi}, \phi]}{\delta\bar{\phi}_i(\tau_1')\delta\bar{\phi}_i(\tau_2')\delta\phi_i(\tau_1)\delta\phi_i(\tau_2)}\Bigg|_{\bar{\phi}=\phi=0}. \tag{24}
$$

In the following, to analyze the phase diagrams of the BFHM, we focus on the saddle-point approximation for the effective action from Eq. (22). Moreover, we point out that this effective action could also be used as a starting point for more general considerations which include the fluctuations around saddle-point approximation. Formally, it can be performed by expanding $G_F^{-1}(i, j, \tau)$ in terms of the $\Delta_i(\tau) - I\phi_i(\tau)$ fields.

C. Saddle-point approximation of the effective action

To investigate the phase diagram which is described by the BFHM effective action from Eq. (22), we apply the mean-field-type approximations.

At first, we rewrite Eq. (22) in the Matsubara frequencies (ω_m, ν_n) and wave-vector (**k**, **q**, **p**) representation, which results in $c_i(\tau) \to c_{\mathbf{k}m}$, $\phi_i(\tau) \to \phi_{\mathbf{q}n}$, $\Delta_i(\tau) \to \Delta_{\mathbf{q}n}$. The Matsubara frequencies are defined as $\omega_m = (2m + 1)\pi/\beta$ and $\nu_n = 2n\pi/\beta$, where $m, n \in \mathbb{Z}$. Then, applying the Bogoliubov-like substitution to the ϕ_{00} and Δ_{00} components, i.e., $\phi_{00} \to \sqrt{N\hbar\beta}\phi_0$ and $\Delta_{00} \to \sqrt{N\hbar\beta}\Delta_0$, and omitting the fluctuating bosonic parts $\Delta_{\mathbf{q}n}$ and $\phi_{\mathbf{q}n}$, the mean-field effective action is obtained, i.e.,

$$
S_{\mathrm{MF}}^{\mathrm{eff}} = \{\epsilon_{\mathbf{0}} - \hbar[G^{1,c}(i\nu_n = 0)]^{-1}\}N\hbar\beta|\phi_0|^2 + \frac{g}{2}(N\hbar\beta)^2|\phi_0|^4 + \frac{N\hbar\beta}{V}|\Delta_0|^2 - \mathrm{Tr}\ln\left[-N\beta G_F^{-1}(i\omega_m, \mathbf{k})\right], \tag{25}
$$

where

$$
G_F^{-1}(\mathbf{k}, i\nu_m) = \begin{bmatrix} i\hbar\omega_m - \xi_{\mathbf{k}} & \Delta_0 - I\phi_0 \\ \bar{\Delta}_0 - I\bar{\phi}_0 & i\hbar\omega_m + \xi_{\mathbf{k}} \end{bmatrix}, \tag{26}
$$

with $\epsilon_{\mathbf{q}} = -2J\sum_\alpha \cos q_\alpha$, $\xi_{\mathbf{k}} = t_{\mathbf{k}} - \mu$, and $t_{\mathbf{k}} = -2t\sum_\alpha \cos k_\alpha$ (symbol $\alpha \in \{x, y, z\}$ denotes Cartesian coordinates). Moreover, in further calculations, we also define coordinate number $z = 6$, which is related to the $\epsilon_{\mathbf{q}}$ by expression $\epsilon_{\mathbf{0}} = -Jz$. Here, we restrict our consideration to the simple cubic lattices. The explicit form of $G^{1,c}(i\nu_n)$ is given in the Appendix. Moreover, in Eq. (25), we use static approximation to the $\Gamma_i^{2,c}$ function and denote this limit by $2g$ (here we do not use the explicit form of g, but it could be found in Ref. [28]).

To describe the ordered phase in terms of ϕ_0 and Δ_0, we calculate the saddle point of the above effective action,

$$
\frac{\partial}{\partial\bar{b}_0}S_{\mathrm{MF}}^{\mathrm{eff}} = 0, \tag{27}
$$

$$
\frac{\partial}{\partial\bar{\Delta}_0}S_{\mathrm{MF}}^{\mathrm{eff}} = 0. \tag{28}
$$

This results in the following coupled equations:

$$
\{\epsilon_{\mathbf{0}} - \hbar[G^{1,c}(i\nu_n = 0)]^{-1}\}\phi_0 + gN\hbar\beta|\phi_0|^2\phi_0 = -\frac{I}{N\hbar\beta}\sum_{m\mathbf{k}} G_F^{12}(\mathbf{k}, i\hbar\omega_m) = -\frac{I}{N}\sum_{\mathbf{k}}\frac{(Vx_0 - I\phi_0)}{2E_{\mathbf{k}}}\tanh\left(\frac{\beta}{2}E_{\mathbf{k}}\right),
$$

$$
x_0 = \frac{1}{N\hbar\beta}\sum_{m\mathbf{k}} G_F^{12}(\mathbf{k}, i\hbar\omega_m) = \frac{1}{N}\sum_{\mathbf{k}}\frac{(Vx_0 - I\phi_0)}{2E_{\mathbf{k}}}\tanh\left(\frac{\beta}{2}E_{\mathbf{k}}\right), \tag{29}
$$

where $Vx_0 = \Delta_0$ and

$$
E_{\mathbf{k}} = \sqrt{\xi_{\mathbf{k}}^2 + |I\phi_0 - Vx_0|^2}. \tag{30}
$$

From Eqs. (29), one immediately sees that x_0 and ϕ_0 are nonlinearly coupled to each other, i.e.,

$$
\{\epsilon_{\mathbf{0}} - \hbar[G^{1,c}(i\nu_n = 0)]^{-1}\}\phi_0 + gN\hbar\beta|\phi_0|^2\phi_0 = -Ix_0, \tag{31}
$$

which suggests that there is only one phase transition from the superfluid phase to the normal phase.

Moreover, it is interesting to point out here that the above equation correctly recovers the limiting cases of noninteracting ($U = 0$) and hard-core ($U \to \infty$) bosons (in which fermionic interaction can be finite, i.e., $V \neq 0$). For $U = 0$, the term with g disappears and one has $\hbar[G^{1,c}(i\nu_n = 0)]^{-1} = \mu^*$, and therefore,

$$
\phi_0 = \frac{-I}{\epsilon_{\mathbf{0}} - (2\mu - 2\Delta_B)}x_0, \tag{32}
$$

which corresponds to the well-known result without a lattice [30]. For $U \to \infty$, two Fock states are taken in Eq. (A1), i.e.,

$n_0 = 0, 1$, which gives $\hbar[G^{1,c}(i\nu_n = 0)]^{-1} = \mu^*/(1 - 2n_{B,0})$ with $n_{B,0} = e^{\beta\mu^*}/(1 + e^{\beta\mu^*})$. Therefore, for the hard-core bosons case, one gets

$$\phi_0 = (Ix_0 + \epsilon_0\phi_0)\frac{1 - 2n_{B,0}}{2\mu - 2\Delta_B}, \tag{33}$$

where we neglect the contribution from the g term by assuming a limit of small order parameter ϕ_0. This result [Eq. (33)] recovers the previous one from Ref. [2].

We have also confirmed that Eqs. (29), in the limit of small amplitude of ϕ_0 (in which the term proportional to g could be neglected), can be recovered from the mean-field and linear response considerations; see the Appendix. Therefore, both of these approaches lead to the same equation for the critical line considered in the rest of the paper.

At the end of this section, it is worth pointing out that the results, obtained in Secs. II B and II C, are quite general and can be used for further analytical and numerical considerations in which I, U, and V interactions are finite quantities. These results are interesting in their own right and can be applied to the study of, e.g., superfluidity or critical phenomena. In our further analysis, we focus on the specific physical regime of the derived theory in which the BHM is set as our reference point.

D. Phase diagram

In this work, we are interested in the phase diagram of the strongly correlated bosonic regime ($J \ll U$). Therefore, at the phase boundary where $x_0 \to 0$, $\phi_0 \to 0$ in Eqs. (29), the critical line is obtained from

$$\epsilon_0 - \hbar G^{-1}(i\nu_n = 0) = \frac{I^2\Pi(T_c)}{1 - V\Pi(T_c)}, \tag{34}$$

where

$$\Pi(T_c) = \frac{1}{N}\sum_{\mathbf{k}}\frac{1}{2\xi_{\mathbf{k}}}\tanh\left(\frac{\xi_{\mathbf{k}}}{2k_B T_c}\right). \tag{35}$$

It is interesting to notice here that in the case of $I = 0$, Eq. (34) and the equation in the second line of (29) get the forms which are known in the phase diagram analysis of the BHM and BCS systems, respectively.

However, in our further analysis, we limit considerations to the case of $V = 0$ for simplicity. Therefore we focus on the pairing mechanism of fermions which comes from the converting interaction I. Then, by direct substitution of $V = 0$ to Eq. (34), the phase boundary in the BFHM is obtained from the equation

$$\epsilon_0 - \hbar G^{-1}(i\nu_n = 0) = I^2\Pi(T_c). \tag{36}$$

In further discussion, we set $\hbar = 1$ and $k_B = 1$ for simplicity.

E. Average particle number

During the analysis of the boson-fermion mixture phase diagram in the following sections, the additional considerations of the average particle number per site n are made; n is calculated within the unperturbed part of the action from Eq. (3) at the phase boundary (it is consistent with the mean-

field calculation of average particle number per site at the phase boundary within the operator approach method; see the Appendix). This means that the zeroth-order partition function has the form $Z_0 = Z_0^F Z_0^B$, where $Z_0^F = \int \mathcal{D}[\bar{c}, c]e^{-S_0^F[\bar{c},c]/\hbar}$ and Z_0^B is defined in Eq. (11). Therefore, n is calculated by using $n = -\partial \ln Z_0/\partial\mu$ and we get

$$n = n_F + 2n_B, \tag{37}$$

where n_F is the average particle number of fermions for both spin components,

$$n_F = 2\sum_{\mathbf{k}}\frac{1}{e^{\beta(t_{\mathbf{k}} - \mu)} + 1}, \tag{38}$$

and n_B is an average particle number of bosons,

$$n_B = \frac{\sum_{n_0=0}^{\infty} n_0 e^{-\beta E_{n_0}}}{\sum_{n_0=0}^{\infty} e^{-\beta E_{n_0}}}, \tag{39}$$

where on-site bosonic energy E_{n_0} is defined in Eq. (A2). There is also a possibility to obtain Eqs. (37)–(39) directly by taking into account Gaussian fluctuations over a saddle-point action $S_{\text{MF}}^{\text{eff}}$ from Eq. (25) at the phase boundary.

It is also worth adding here that an improved approach, which includes the effect of resonant interaction I, bosonic hopping J, and fermionic interaction V, in the normal phase, can be achieved by using the self-consistent T-matrix theory [15,23].

III. RESULTS AND DISCUSSION

A. Phase diagram of the BHM

In order to clarify further discussion, we briefly review the finite-temperature phase diagram of the standard BHM in terms of reduced critical temperature T_c/zJ versus average concentration of bosons per site n_B.

Using previously defined bosonic annihilation and creation operators b_i and $b_i^\dagger$, the BHM Hamiltonian has the form $H_{\text{BHM}} = -\sum_{ij}(J_{ij} + \mu\delta_{ij})b_i^\dagger b_j + U\sum_i b_i^\dagger b_i^\dagger b_i b_i$. The phase diagram comprising the SF, bosonic Mott insulator (BMI), and normal (N) phases is well known [36–38] and, in the mean-field approximation, the critical line is given by $\epsilon_0 - [G^{1,c}(i\nu_n = 0)]^{-1} = 0$. In Fig. 1, we plot the critical temperature T_c/zJ dependence on the average density of bosons per site n_B for the critical boundary in the BHM. The BMI for different integer values of n_B is located only between lobes at zero temperatures, which are indicated in Fig. 1 by black arrows (at finite temperatures, there is no true insulating state [39]). Here and in the following section, we choose $U/Jz = 20$ to analyze the strong interaction limit of bosonic particles.

B. Density phase diagram of the BFHM model

We are interested in the density phase diagram of the BFHM in the limit $J \ll U$ and $V = 0$ (as was mentioned in Sec. II D). The critical boundary line at finite temperatures is obtained from Eq. (36). In the following Secs. III C, III D, and III E, the phase diagram of the BFHM is analyzed in three different regimes, respectively, of parameter Δ_B which controls the mutual position of the fermionic and bosonic band, namely, (a) $\Delta_B/zt = 0$, (b) $\Delta_B/zt > 0$, and (c) $\Delta_B/zt < 0$. In particular,
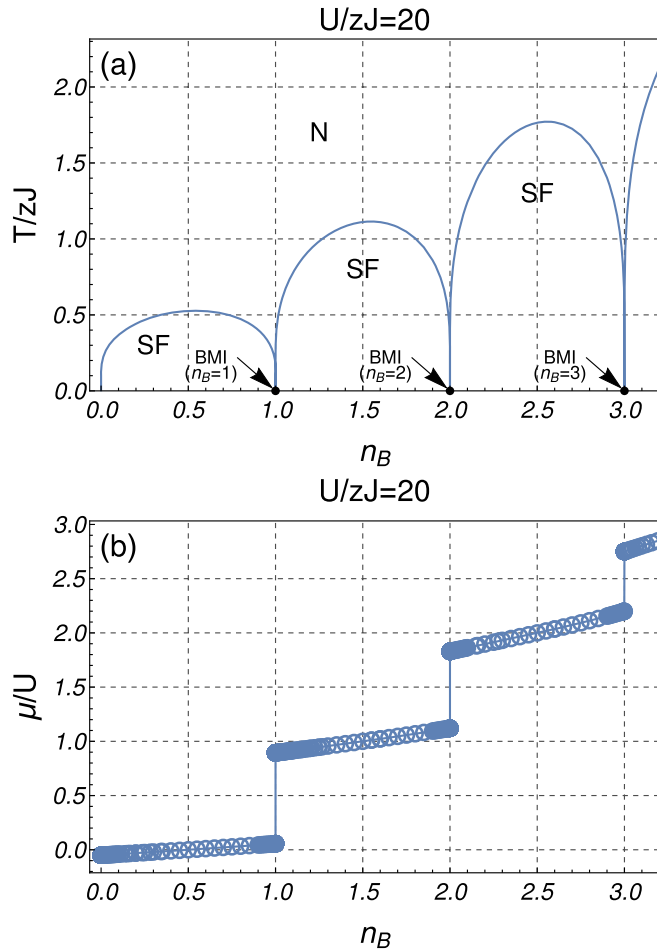
FIG. 1. (a) Mean-field phase diagram of the BHM (temperature T/Jz vs average particle number per site n_B). (b) Chemical potential μ/U vs n_B calculated along the critical line from (a). For clarity, the circles are added on the numerical data points in (b).
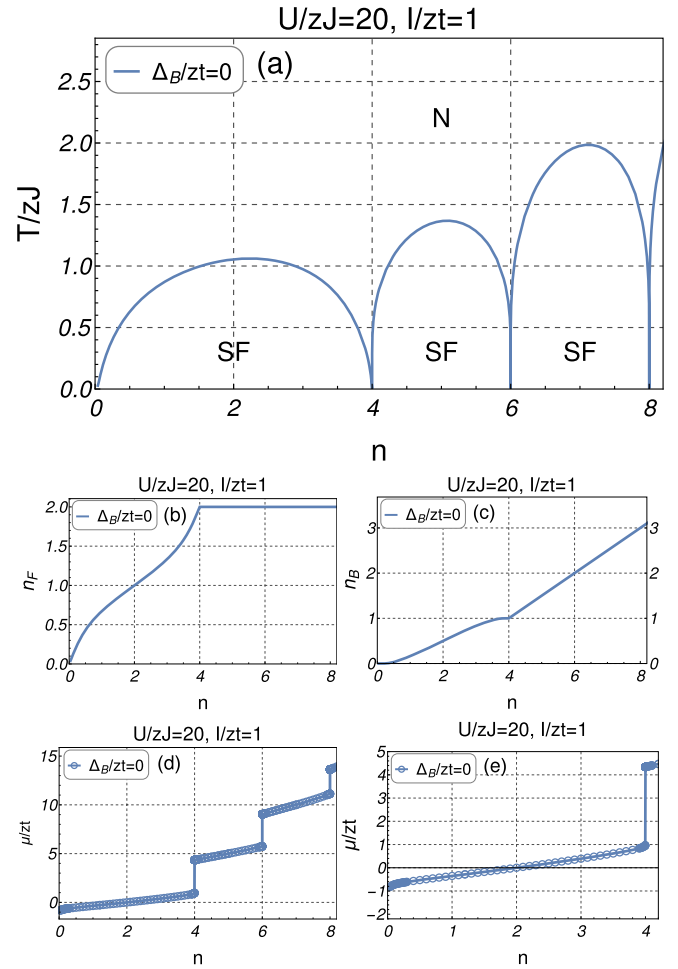

FIG. 2. (a) Finite-temperature mean-field phase diagram of the BFHM vs total particle number per site $n = 2n_B + n_F$ for zero detuning of parameter Δ_B. (b)–(d) Plots of n_F, n_B, and μ/zt, respectively, vs n [the obtained data are evaluated along the critical line from (a)]. (e) An enlargement of the vicinity of zero chemical potential from (d). Plots are made assuming that $U/zJ = 20$, $I/zt = 1$, $J = t/2$. For clarity, the circles are added on the numerical data points in (d) and (e).

the value of parameter Δ_B is directly related to the position of the bottom of the bosonic band with respect to that of the fermionic one. It is clear from considering the BFHM Hamiltonian from Eq. (1) and from relation $J = t/2$, which corresponds to the assumption that one molecule is made of two fermionic particles. The bottom of the boson band is located at the center of the fermion band at $\Delta_B/zt = 0.25$ and it starts to appear below the fermionic band for $\Delta_B/zt < -0.75$ and above for $\Delta_B/zt > 1.25$.

C. Zero detuning ($\Delta_B = 0$)

In Fig. 2, we show the finite-temperature phase diagram for the BFHM with zero detuning $\Delta_B/zt = 0$, finite bosonic interaction strength $U/zJ = 20$, and converting interaction $I/zt = 1$. These results explicitly show that if the $\Delta_B/zt = 0$ parameter is close to the $\Delta_B/zt = 0.25$ value (i.e., the bottom of the bosonic band is close to the middle of the fermionic one), then the critical line assumes a regular lobe structure, similar to the phase diagram of the standard BHM (see Fig. 1). However, in the BFHM case, the lowest lobe is relatively wider than the others [i.e., $n \in (0,4)$ instead of width 2 in n units in

comparison to the pure BHM case; see Fig. 1]. This widening is related to the gradual filling up of the fermionic band with increasing value of total particles n [see Fig. 2(b)]. Indeed, the chemical potential gradually crosses the fermionic band, which is clearly visible in Figs. 2(d) and 2(e), i.e., μ/zt appear at the bottom of the fermionic band ($\mu = -zt$) at $n = 0$ and end at the top of the fermionic band ($\mu = zt$) for $n = 4$.

It is interesting to notice here that in comparison to the BHM case (Fig. 1), there is an enhancement of the superfluid critical temperature when $I \neq 0$. Starting from the second lobe, this enhancement can be simply accounted for by the pairing mechanism of fermionic holes. This is confirmed by the slight deviations of fermionic density from a band insulator regime ($n_F = 2$) for $n > 4$ [see Fig. 2(b) and its corresponding enlargement in Fig. 3].

The above picture is dramatically changed when detuning starts to deviate from zero value. It will be discussed below.
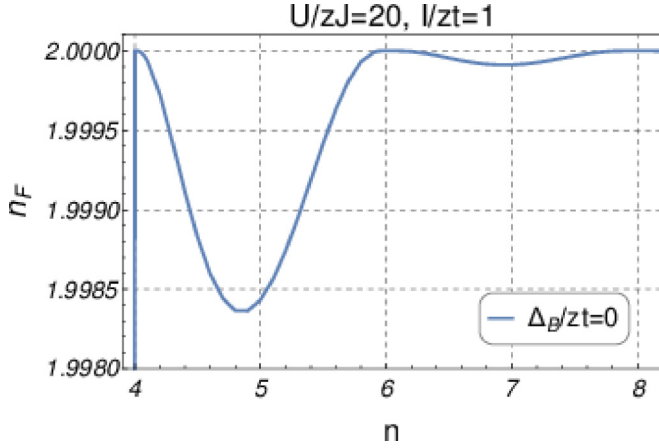
FIG. 3. Dependence of fermionic density n_F on the total particle density n. This figure is an enlargement of the $n \in (4,8)$ region from Fig. 2(b).

D. Positive detuning ($\Delta_B > 0$)

With increasing value of the Δ_B/zt parameter, the bottom of the bosonic band is above the fermionic one for $\Delta_B/zt > 1.25$. This should result in increasing the fermionic density at the expense of the bosonic one at low n, which indeed is clearly visible in Figs. 4(a)–4(c). In particular, with increasing Δ_B/zt, the lower part of the first lobe gradually diminishes and the first lobelike structure appears for $n \in (2,4)$ (see Fig. 4 with $\Delta_B/zt = 1.5$). Such a situation is also confirmed by analysis of the chemical potential μ/zt [see Figs. 4(d) and 4(e)], which shows that its value starts to appear only in the region of the fermionic band for $n \in (0,2)$ and for higher values of Δ_B/zt for which the bosonic density is very low [it should be compared to the situation with $\Delta_B/zt = 0$ in which $\mu \in \langle -zt, zt \rangle$ for $n \in (0,4)$; see Figs. 4(d) and 4(e)].

E. Negative detuning ($\Delta_B < 0$)

The situation is even more interesting for negative detuning for which the bottom of the bosonic band is below the fermionic one for $\Delta_B/zt < -0.75$. Intuitively, when the number of particles n is increased, at first the bosonic band should start to fill up. This intuition fully agrees with our simulation presented in Fig. 5 for n_B and n_F versus n, and is clearly observed in the regime of relatively high negative values of $\Delta_B/zt = -2.5$. However, in comparison to the reference case at $\Delta_B/zt = 0$, the situation here is more complex, and the critical line at $\Delta_B/zt = -2.5$ for the $n \in \langle 0,4 \rangle$ range decays into two lobes [see Fig. 5(a)]. The first lobe at $n \in \langle 0,2 \rangle$ contains the SF phase with gradually increasing average number of bosonic particles n_B [Fig. 5(c)] and the second lobe at $n \in \langle 2,4 \rangle$ is characterized by the almost integer bosonic density n_B (here close to one), i.e., it has the BMI character for bosonic particles (the bosonic density deviates from the integer number with order less than 10^{-6}) [see Fig. 5(c)]. Moreover, the fermionic part for $n \in \langle 2,4 \rangle$ gradually changes its density from $n_F = 0$ to $n_F = 2$ with increasing value of n. We also clearly see that the phase is characterized by the location of the chemical potential inside the fermionic band, pointing out that the system is at the Feshbach resonance [see Figs. 5(d) and 5(e)]. Further, we
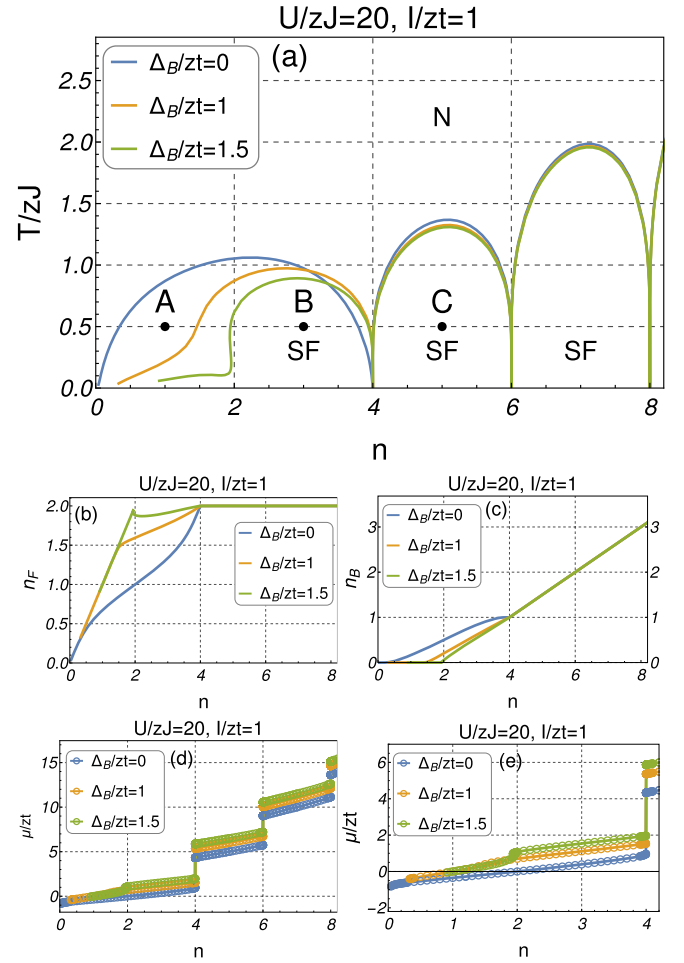

FIG. 4. (a) Finite-temperature mean-field phase diagram of the BFHM vs total particle number per site $n = 2n_B + n_F$ for different strengths of detuning Δ_B (see legend). (b)–(d) Plots of n_F, n_B, and μ/zt, respectively, vs n [the obtained data are evaluated along the critical line from (a)]. (e) An enlargement of the vicinity of zero chemical potential from (d). Plots are made assuming that $U/zJ = 20$, $I/zt = 1$, $J = t/2$. For comparison, we plot $\Delta_B/zt = 0$ from Fig. 2. For clarity, the circles are added on the numerical data points in (d) and (e). The meaning of the A, B, and C points is given in Sec. III F.

argue that this superfluid phase with number of bosons close to integer value arises purely from the resonant mechanism and, for simplicity, we denote it as the resonant superfluid (RSF) phase.

To show the resonant character of the RSF, we check the sensitivity of this phase by tuning the amplitude of the converting interaction in S_0^{FB} from Eq. (3). Namely, in Fig. 6, we plot the phase diagram for different values of I/zt. This phase diagram shows that the RSF phase is highly suppressed at finite temperatures and it almost disappears for $I/zt = 0.5$. Therefore, one can conclude that the RSF phase originates from the Feshbach-like correlations.

Moreover, it is worth adding here that fermionic n_F and bosonic n_B densities are almost intact with respect to the change of I/zt in the RSF phase [see Figs. 6(b), 6(c) and 7]. However, as expected, we observe that there is a slight change
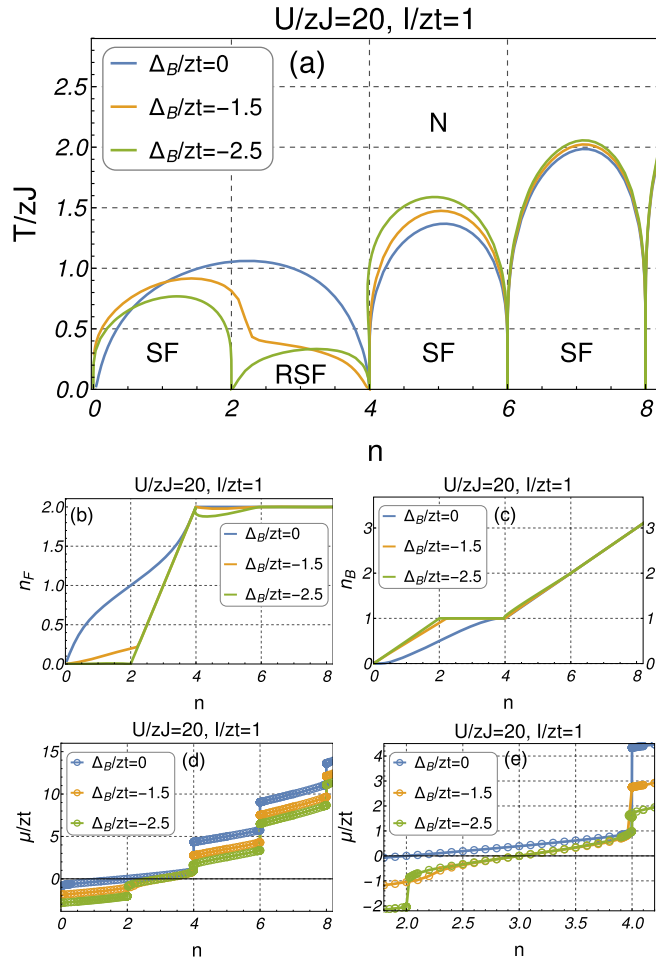
FIG. 5. (a) Finite-temperature mean-field phase diagram of the BFHM vs total particle number per site $n = 2n_B + n_F$ for different strengths of detuning parameter Δ_B (see legend). (b)–(d) Plots of n_F, n_B, and μ/zt, respectively, vs n [the obtained data are evaluated along the critical line from (a)]. (e) An enlargement of the vicinity of zero chemical potential from (d). Plots are made assuming that $U/zJ = 20$, $I/zt = 1$, $J = t/2$. For comparison, we plot $\Delta_B/zt = 0$ from Fig. 2. For clarity, the circles are added on the numerical data points in (d) and (e).
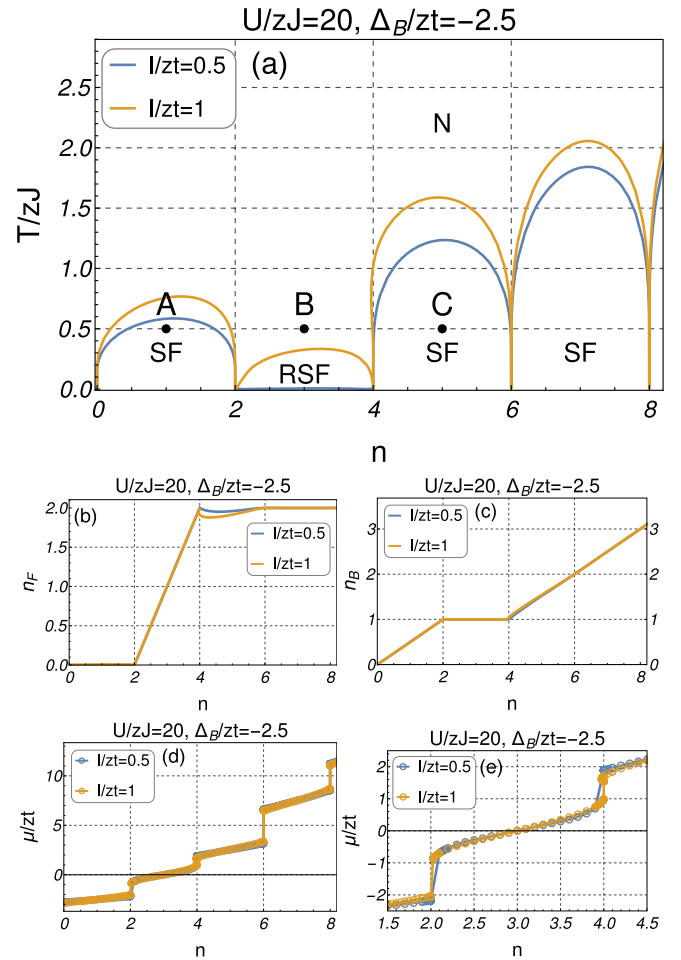
FIG. 6. (a) Finite-temperature mean-field phase diagram of the BFHM vs total particle number per site $n = 2n_B + n_F$ for different strengths of converting interaction I/zt (see legend). (b)–(d) Plots of n_F, n_B, and μ/zt, respectively, vs n [the obtained data are evaluated along the critical line from (a)]. (e) An enlargement of the vicinity of zero chemical potential from (d). Plots are made assuming that $U/zJ = 20$, $\Delta_B/zt = -2.5$, $J = t/2$. For clarity, the circles are added on the numerical data points in (d) and (e). The meaning of the A, B, and C points is given in Sec. III F.

of these densities not visible in the presented density plots (the order of this change is less than 10^{-6}).

We also checked the vicinity of the RSF region by analyzing the normal phase above the critical temperature in terms of n_F and n_B densities at a constant n (see Fig. 8). These densities correspond to the $I/zt = 0$ regime at this level of approximation (see Sec. II E and Eqs. (37)–(39). From Fig. 8, we observe that in the $T \to 0$ limit, n_B is pinned to the integer value equal to one, while n_F gradually increases for the corresponding total particle density $n = 2, 3, 4$. This observation is consistent with the conclusion about the RSF phase drawn in the previous paragraph.

It is also worth adding here that the above picture of the BFHM phase diagram is also consistent with the work in Ref. [40], which considered the hard-core limit of bosonic particles without bosonic hopping ($J = 0$). It should not be surprising because our theory properly recovers this limit at

the mean-field level [see Eq. (33)]. However, the RSF phase with the number of bosons close to one is a different behavior which appears beyond the hard-core limit.

Moreover, when the system is beyond the Feshbach resonance for $\Delta_B/zt = -2.5$ (i.e., the chemical potential is below or above the fermionic band), there is another interesting feature, observed in Fig. 6. Namely, the SF phase is favored for $n \in (0, 2)$ and $n > 4$, but it is important to point out here that the mechanism behind it is quite different. In the $n \in (0, 2)$ range, the SF is enhanced through paring of fermionic particles (BCS-like character), but in the $n > 4$ range, the pairing mechanism is through fermionic holes. It is indicated by the corresponding low-magnitude enhancement [for $n \in (0, 2)$] or reduction (for $n > 4$) of the fermionic density part in numerical data.

At the end of this section, we would like to also add that for higher values of negative detuning Δ_B/zt, the general behavior of the phase boundary is similar to that discussed above.
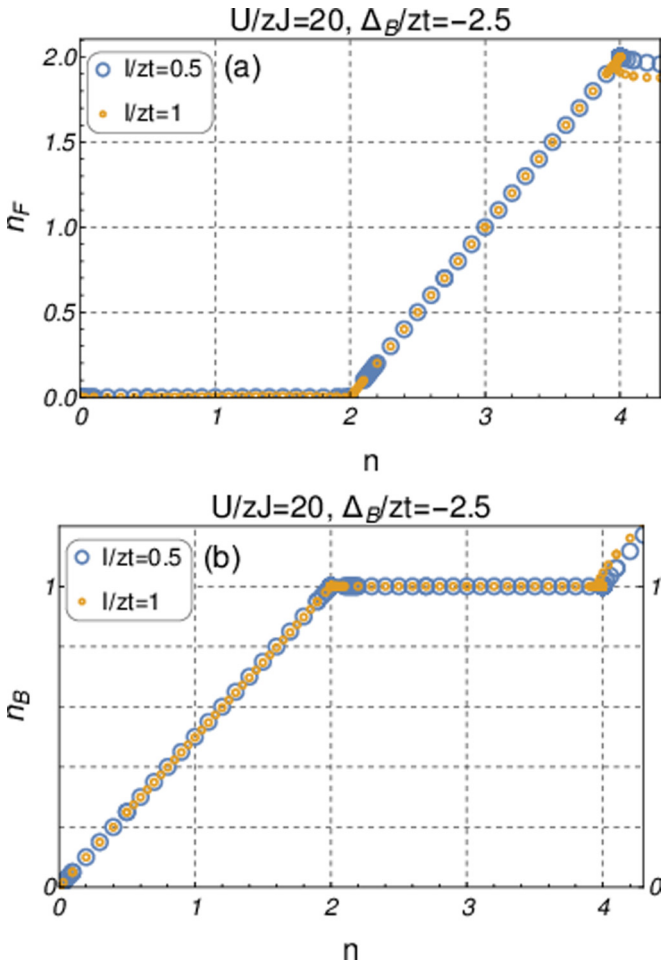
FIG. 7. (a), (b) Enlargements of the relevant parts of Figs. 6(b) and 6(c), respectively.
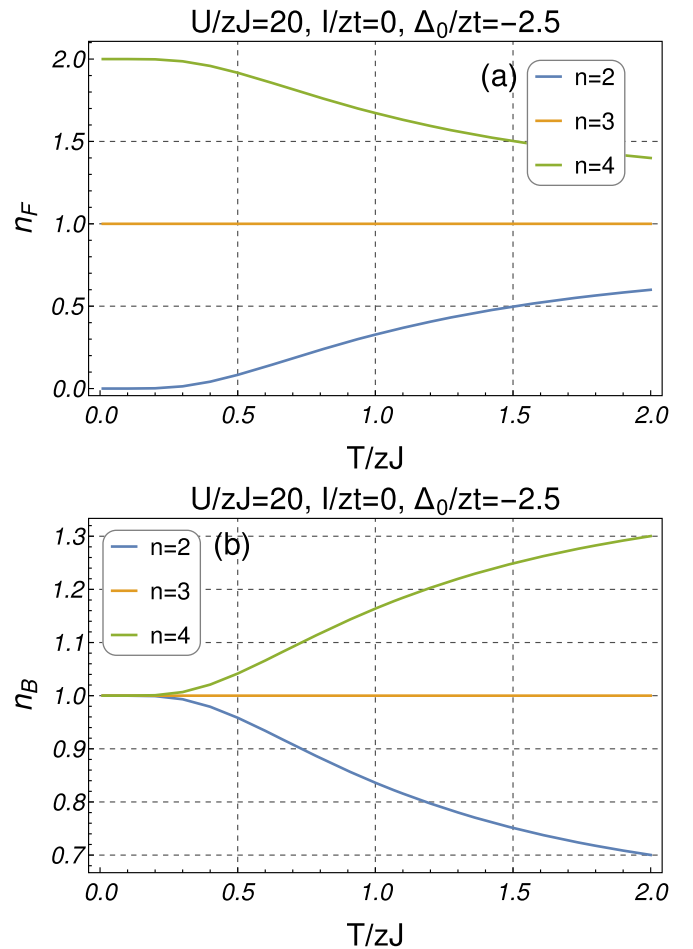

FIG. 8. (a) Fermionic n_F and (b) bosonic n_B average particle density per site with fixed total number of particles $n = n_F + 2n_B$ [see Eqs. (37)–(39)]. The other parameters are $U/zJ = 20$, $J = t/2$.

Namely, higher negative values of Δ_B/zt shift the chemical potential also to higher negative values, causing the Feshbach resonance region around $\mu/zt \in \langle -1, 1 \rangle$ to appear for higher densities. Then, depending on the Δ_B/zt value, a situation like that in the former cases appears, i.e., (1) the widening of one of the lobes such as for $\Delta_B/zt = 0$ (see Fig. 4) or (2) the emergence of RSF mixture such as for $\Delta_B/zt = -2.5$ (see Fig. 5). In particular, up to $\Delta_B/zt = -10$ with the same BFHM Hamiltonian parameters as before, we numerically check that the first situation (1) appears for $\Delta_B/zt = -5$ and $\Delta_B/zt = -10$ and the second one (2) appears for $\Delta_B/zt = -7.5$ [here, the RSF phase emerge for $n \in (4, 6)$].

It would also be interesting in further investigations, beyond the mean-field approximation, to include the effects of pairing fluctuations into theory which should imply lowering of the superfluid critical temperature. Then the temperature obtained in this work will correspond to the appearance of the pseudogap regime for fermionic particles [9,15,23].

F. RSF phase in the time-of-flight-type experiment

Time-of-flight (TOF)-type spectroscopy is one of the most powerful methods of measurements in the state-of-the-art current experimental setups in ultracold atoms. Within the optical lattice systems, it has been widely used for, e.g., bosons [41–45], fermions [46,47], or boson-fermion mixtures [48,49]. In particular, it is relatively simple to probe coherence via momentum distribution encoded in a freely expanding cloud. As an example, it has been previously used to detect the SF-BMI quantum phase transition in the bosonic Rb atoms [45] or resonant superfluidity in the fermionic Li atoms [47]. In a realistic experiment, the enhancement of coherence is observed as the appearance of peaks in the time-of-flight pattern [41,44,45,47].

We suggest that the footprint of the RSF phase can be tested by preparing an ultracold fermionic gas at the Feshbach resonance with negative detuning of the Δ_B parameter. The detuning should be about two-and-a-half-times greater than the width of the fermionic band. Then, by repeating the experiment with increasing number of fermions which simulate the BFHM (which is close to the ground state), one should observe a lowering of coherence at $n \in \langle 2, 4 \rangle$ densities. It can be deduced from the phase diagram in Fig. 6 where, in the range $n \in (0, 2)$ and $n > 4$, the SF phase has a higher critical temperature than in the $n \in (2, 4)$ region.

For instance, let us assume that the atomic gas is prepared at similar temperatures for different particle numbers which are represented by points A, B, and C in Figs. 4(a) and 6(a). Furthermore, let us assume that in each of these phases represented by points A, B, and C, a TOF experiment is performed. Then, it can be concluded that for the situation with positive detuning, as in Fig. 4(a), the coherence of bosonic particles should be an increasing function of n at corresponding points A, B, and C because of the deeper penetration of the system into the SF phase for A, B, and C, respectively. However, this situation should be quite different for negative detuning of Δ_B/zt. As shown in Fig. 6(a), point B in comparison to points A and C is located beyond the SF phase, which means that the TOF pattern does not exhibit the behavior characteristic of the SF phase [37]. Therefore, for negative detuning, one should observe nonmonotonous behavior of the coherence peaks, which can be read off from the TOF patterns for the corresponding points A, B, and C. Moreover, increasing the strength of Feshbach interaction I/zt should result in the gradual disappearance of this nonmonotonous behavior at point B [see Fig. 6(a)]. Consequently, such coherence dependence, which can be observed in experiment, could be accounted for by the appearance of the RSF phase in the investigated system.

IV. SUMMARY

In this work, we investigated the limit of strongly correlated Feshbach molecules at finite temperatures in a three-dimensional lattice. We show that for negative detuning Δ_B/zt and at least for weak strength of converting interaction I/zt, a resonant superfluid phase (RSF) appears which is characterized by an arbitrary number of fermions per site (i.e., fermionic concentration between 0 and 2) and an integer number of bosonic atoms. This happens when fermions are in the Feshbach resonance. We show that this resonant character of the RSF phase is unstable toward weakening converting interaction I/zt. In the situation when the fermions are beyond resonance, the superfluid phase is strengthened. We explain that this enhancement is caused by a hole-pairing mechanism for higher densities, while for lower densities, it is a standard fermionic particle pairing mechanism, which corresponds to that known in the BCS theory.

Moreover, we have also discussed the experimental protocol in which the footprint of the RSF phase can appear in a TOF-type experiment. Namely, the footprint of the RSF phase could be simply observed as a nonmonotonous behavior of coherence peaks from the time-of-flight pattern when the number of fermions is increased.

In future investigations, it will also be interesting to study the system's behavior from the point of view of tuning the parameter Δ_B at fixed total n. An especially interesting analysis would be for the total density equal to two ($n = 2$) in which two different peculiar regimes should appear depending on the Δ_B and U amplitude. Namely, tuning the system from a positive $\Delta_B > 0$ to a negative $\Delta_B < 0$ value should result in a transition from a fermionic band insulator ($n_F = 2, n_B = 0$) to a SF phase, and from a SF to bosonic Mott insulator ($n_F = 0$, $n_B = 1$). We leave this problem for future studies in which careful analysis of the BFHM ground state is also required.

APPENDIX

1. Local Green function

The on-site single-particle Green function, defined as $\frac{1}{\hbar} G^{1,c}(\tau - \tau') = -\langle \bar{\psi}_i(\tau) \psi_i(\tau') \rangle_0^B$, is given by

$$\frac{1}{\hbar} G^{1,c}(i\nu_n) = \frac{1}{Z_0} \sum_{n_0=0}^{\infty} (n_0 + 1) \frac{e^{-\beta E_{n_0+1}} - e^{-\beta E_{n_0}}}{E_{n_0+1} - E_{n_0} - i\hbar\nu_n} , \quad \text{(A1)}$$

where

$$E_{n_0} = -\mu^* n_0 + U n_0(n_0 - 1)/2 , \quad \text{(A2)}$$

$$Z_0 = \sum_{n_0=0}^{\infty} e^{-\beta E_{n_0}} . \quad \text{(A3)}$$

2. Generating functional in the BFHM

The generating function of the statistical sum from Eq. (2) has the form

$$Z[\bar{\gamma}, \gamma] = \int \mathcal{D}[\bar{c}, c, \bar{b}, b] e^{\sum_{ij} \int_0^{\hbar\beta} d\tau J_{ij} \bar{b}_i(\tau) b_j(\tau) - S_0^F[\bar{c}, c] - S_0^B[\bar{b}, b] - S_0^{FB}[\bar{b}, b, \bar{c}, c] + \sum_i \int_0^\beta d\tau [\bar{\gamma}_i(\tau) b_i(\tau) + \text{c.c.}]} , \quad \text{(A4)}$$

where $\gamma_i(\tau)$, $\bar{\gamma}_i(\tau)$ are external sources. It can be rewritten to the form

$$Z[\bar{\gamma}, \gamma] = \int \mathcal{D}[\bar{c}, c, \bar{b}, b] e^{\sum_{ij} \int_0^{\hbar\beta} d\tau J_{ij} \bar{b}_i(\tau) b_j(\tau) - S_0^F[\bar{c}, c] - S_0^B[\bar{b}, b] - \sum_i \int_0^\beta d\tau \{[-\bar{\psi}_i(\tau) + I\bar{c}_{i\uparrow}(\tau)\bar{c}_{i\downarrow}(\tau) - \bar{\gamma}_i(\tau)] b_i(\tau) + \text{c.c.}\}} . \quad \text{(A5)}$$

After the first HS of bosonic fields $b_i(\tau)$, $\bar{b}_i(\tau)$ [see also Eq. (9)], one has

$$Z[\bar{\gamma}, \gamma] = Z_0^B \det[\mathbf{J}^{-1}] \int \mathcal{D}[\bar{c}, c, \bar{\psi}, \psi] e^{-\frac{1}{\hbar} \sum_{ij} \int_0^{\hbar\beta} d\tau J_{ij}^{-1} \bar{\psi}_i(\tau) \psi_j(\tau) - \frac{1}{\hbar} \sum_i \int_0^{\hbar\beta} d\tau \{[-\bar{\psi}_i(\tau) + I\bar{c}_{i\uparrow}(\tau)\bar{c}_{i\downarrow}(\tau) - \bar{\gamma}_i(\tau)] b_i(\tau) + \text{c.c.}\}}$$
$$\times e^{-S_0^F[\bar{c}, c] - S_0^B[\bar{b}, b] - S_0^{FB}[\bar{b}, b, \bar{c}, c]} . \quad \text{(A6)}$$

Next, shifting $\psi_i(\tau) \to \psi_i(\tau) - \gamma_i(\tau) + Ic_{i\downarrow}(\tau)c_{i\uparrow}(\tau)$, $\bar{\psi}_i(\tau) \to \bar{\psi}_i(\tau) - \bar{\gamma}_i(\tau) + I\bar{c}_{i\uparrow}(\tau)\bar{c}_{i\downarrow}(\tau)$, we obtain

$$Z = Z_0^B \det[\mathbf{J}^{-1}] \int \mathcal{D}[\bar{c}, c, \bar{\psi}, \psi] e^{-\frac{1}{\hbar}\sum_{ij}\int_0^{\hbar\beta} d\tau J_{ij}^{-1}[\bar{\psi}_i(\tau)+I\bar{c}_{i\uparrow}(\tau)\bar{c}_{i\downarrow}(\tau)-\bar{\gamma}_i(\tau)][\psi_j(\tau)+Ic_{j\downarrow}(\tau)c_{j\uparrow}(\tau)-\gamma_i(\tau)]-W_1[\bar{\psi},\psi]} e^{-S_0^F[\bar{c},c]}. \quad (A7)$$

Finally, taking the second HS [see also Eq. (18)],

$$-\sum_{ij}\int_0^{\hbar\beta} d\tau[\bar{\psi}_i(\tau)+I\bar{c}_{i\uparrow}(\tau)\bar{c}_{i\downarrow}(\tau)-\bar{\gamma}_i(\tau)]J_{ij}^{-1}[\psi_j(\tau)+Ic_{j\downarrow}(\tau)c_{j\uparrow}(\tau)-\gamma_i(\tau)] \to \sum_{ij}\int_0^{\hbar\beta} d\tau J_{ij}\bar{\phi}_i(\tau)\phi_j(\tau)$$

$$-\left\{\sum_i\int_0^{\hbar\beta} d\tau\bar{\phi}_i(\tau)[\psi_i(\tau)+Ic_{i\downarrow}(\tau)c_{i\uparrow}(\tau)-\gamma_i(\tau)]+\text{c.c.}\right\}, \quad (A8)$$

we have

$$Z[\bar{\gamma},\gamma] = Z_0^B \det[\mathbf{J}^{-1}]\det[-\mathbf{J}]\int \mathcal{D}[\bar{c},c,\bar{\psi},\psi,\bar{\phi},\phi] e^{\sum_{ij}\int_0^{\hbar\beta} d\tau J_{ij}\bar{\phi}_i(\tau)\phi_j(\tau)+\sum_i\int_0^{\hbar\beta} d\tau\{\bar{\phi}_i(\tau)\psi_i(\tau)+\text{c.c.}\}}$$

$$\times e^{-\frac{1}{\hbar}W_1[\bar{\psi},\psi]+\tilde{S}_0^F[\bar{c},c,\bar{\Delta},\Delta]+\sum_i\int_0^{\hbar\beta} d\tau\{\bar{\phi}_i(\tau)\gamma_i(\tau)+\text{c.c.}\}}. \quad (A9)$$

From Eqs. (A4) and (A9), we see that the $b_i(\tau)$, $\bar{b}_i(\tau)$ and $\phi_i(\tau)$, $\bar{\phi}_i(\tau)$ fields have the same generating functional $Z[\bar{\gamma}, \gamma]$. The above considerations about generating the functional correspond to those in Appendix A of Ref. [28].

3. Mean-field equations for order parameters: The operator approach

Equations (29) were derived by using a coherent-state path integral within a double Hubbard-Stratonovich transformation within the bosonic part of the action. Now, we show that these equations can also be recovered by using a standard operator approach, at least in the small-ϕ_0 limit. In order to get the equations for order parameters ϕ_0 and x_0, we start from the mean-field approximation applied to the BFHM Hamiltonian defined in Eq. (1), i.e., for the bosonic hopping term,

$$-\sum_{ij} J_{ij}b_i^\dagger b_j \approx NzJ|\phi_0|^2 - zJ\phi_0\sum_i b_i^\dagger - zJ\bar{\phi}_0\sum_i b_i, \quad (A10)$$

for the fermionic interaction term (BCS-type approximation in the pairing channel),

$$V\sum_i c_{i\uparrow}^\dagger c_{i\downarrow}^\dagger c_{i\downarrow} c_{i\uparrow} \approx \frac{V}{N}\sum_{\mathbf{k}\mathbf{k}'} c_{\mathbf{k}'\uparrow}^\dagger c_{-\mathbf{k}'\downarrow}^\dagger c_{-\mathbf{k}\downarrow} c_{\mathbf{k}\uparrow}$$

$$\approx -\frac{N}{V}|\Delta_0|^2 + \sum_{\mathbf{k}}\bar{\Delta}_0 c_{-\mathbf{k}\downarrow}c_{\mathbf{k}\uparrow}$$

$$+\sum_{\mathbf{k}'} c_{\mathbf{k}'\uparrow}^\dagger c_{-\mathbf{k}'\downarrow}^\dagger \Delta_0, \quad (A11)$$

and for resonant interaction term,

$$I\sum_i(c_{i\uparrow}^\dagger c_{i\downarrow}^\dagger b_i + b_i^\dagger c_{i\downarrow}c_{i\uparrow}) \approx I\sum_{\mathbf{k}}(c_{\mathbf{k}\uparrow}^\dagger c_{-\mathbf{k}\downarrow}^\dagger \phi_0 + \bar{\phi}_0 c_{-\mathbf{k}\downarrow}c_{\mathbf{k}\uparrow})$$

$$+I\frac{1}{V}\sum_i(\bar{\Delta}_0 b_i + \Delta_0 b_i^\dagger)$$

$$-I\frac{1}{V}\sum_i(\bar{\Delta}_0\phi_0 + \Delta_0\bar{\phi}_0). \quad (A12)$$

Then, the thermodynamic potential can be written in the form

$$\Omega = -\frac{1}{\beta}\ln Z, \quad (A13)$$

with

$$Z = \text{Tr}\, e^{-\beta\left(H_{\text{eff}}^F + H_{\text{eff}}^B + H_{\text{eff}}^{\text{FB}}\right)},$$

and where

$$H_{\text{eff}}^F = \sum_{\mathbf{k}\sigma}\xi_{\mathbf{k}}c_{\mathbf{k}\sigma}^\dagger c_{\mathbf{k}\sigma} - \sum_{\mathbf{k}}(\bar{\Delta}_0 - I\bar{\phi}_0)c_{-\mathbf{k}\downarrow}c_{\mathbf{k}\uparrow}$$

$$-\sum_{\mathbf{k}}c_{\mathbf{k}\uparrow}^\dagger c_{-\mathbf{k}\downarrow}^\dagger(\Delta_0 - I\phi_0) + \frac{N}{V}|\Delta_0|^2, \quad (A14)$$

$$H_{\text{eff}}^B = NzJ|\phi_0|^2 + \left(I\frac{1}{V}\Delta_0 - zJ\phi_0\right)\sum_i b_i^\dagger$$

$$+\left(I\frac{1}{V}\bar{\Delta}_0 - zJ\bar{\phi}_0\right)\sum_i b_i - \sum_i \mu^* b_i^\dagger b_i$$

$$+U\sum_i b_i^\dagger b_i^\dagger b_i b_i, \quad (A15)$$

$$H_{\text{eff}}^{\text{FB}} = -I\frac{N}{V}(\bar{\Delta}_0\phi_0 + \Delta_0\bar{\phi}_0). \quad (A16)$$

Next, the ϕ_0 and Δ amplitudes can be obtained from the conditions

$$\frac{\partial\Omega}{\partial\bar{\Delta}_0} = 0, \quad \frac{\partial\Omega}{\partial\bar{\phi}_0} = 0, \quad (A17)$$

which give

$$0 = -\frac{N}{V}\Delta_0 + I\frac{N}{V}\phi_0 + \sum_{\mathbf{k}}\langle c_{-\mathbf{k}\downarrow}c_{\mathbf{k}\uparrow}\rangle - \frac{I}{V}\sum_i\langle b_i\rangle,$$

$$0 = -I\sum_{\mathbf{k}}\langle c_{-\mathbf{k}\downarrow}c_{\mathbf{k}\uparrow}\rangle - NzJ\phi_0 + zJ\sum_i\langle b_i\rangle + I\frac{N}{V}\Delta_0. \quad (A18)$$

This leads to

$$x_0 = \frac{1}{N} \sum_{\mathbf{k}} \langle c_{-\mathbf{k}\downarrow} c_{\mathbf{k}\uparrow} \rangle, \tag{A19}$$

$$\phi_0 = \frac{1}{N} \sum_i \langle b_i \rangle, \tag{A20}$$

where in this section the statistical average is defined as $\langle \cdot \rangle = \mathrm{Tr} \ldots e^{-\beta(H_{\mathrm{eff}}^{\mathrm{fer}} + H_{\mathrm{eff}}^{\mathrm{bos}} + H_{\mathrm{eff}}^{\mathrm{fer-bos}})}/Z$ and we introduce $x_0 = \Delta/V$, which is the same as in Sec. II C.

Now we focus on the first equation, i.e., Eq. (A19). The expectation value $\langle c_{-\mathbf{k}\downarrow} c_{\mathbf{k}\uparrow} \rangle$ for a given wave vector $\mathbf{k}$ can be calculated by diagonalizing the $H_{\mathrm{eff}}^{\mathrm{fer}}$ Hamiltonian using the standard Bogoliubov transformation,

$$c_{\mathbf{k}\uparrow} = \bar{u}_{\mathbf{k}} \gamma_{\mathbf{k}\uparrow} + \bar{v}_{\mathbf{k}} \gamma_{-\mathbf{k}\downarrow}^{\dagger}, \tag{A21}$$

$$c_{\mathbf{k}\downarrow} = \bar{u}_{\mathbf{k}} \gamma_{\mathbf{k}\downarrow} - \bar{v}_{\mathbf{k}} \gamma_{-\mathbf{k}\uparrow}^{\dagger}, \tag{A22}$$

with

$$|u_{\mathbf{k}}|^2 = \frac{1}{2}\left(1 + \frac{\xi_{\mathbf{k}}}{E_{\mathbf{k}}}\right), \tag{A23}$$

$$|v_{\mathbf{k}}|^2 = \frac{1}{2}\left(1 - \frac{\xi_{\mathbf{k}}}{E_{\mathbf{k}}}\right). \tag{A24}$$

Then we obtain

$$\langle c_{-\mathbf{k}\downarrow} c_{\mathbf{k}\uparrow} \rangle = \frac{V x_0 - I\phi_0}{2E_{\mathbf{k}}} \tanh\left(\frac{\beta}{2} E_{\mathbf{k}}\right), \tag{A25}$$

with a quasiparticle fermionic energy $E_{\mathbf{k}}$ defined as before in Eq. (30).

For the next equation, i.e., Eq. (A20), we calculate by using the linear response theory. Assuming that the ϕ_0 and x_0 amplitudes are small, one can expand $\langle b_i \rangle$ in terms of these parameters, which gives

$$\frac{1}{N} \sum_i \langle b_i \rangle \approx -\frac{1}{\hbar} z J \phi_0 G^{1,c}(i\nu_n = 0) + \frac{1}{\hbar} I x_0 G^{1,c}(i\nu_n = 0). \tag{A26}$$

Finally, combining Eqs. (A19), (A20), (A25), and (A26), one gets

$$\{\epsilon_0 - \hbar[G^{1,c}(i\nu_n = 0)]^{-1}\}\phi_0$$
$$= -\frac{I}{N} \sum_{\mathbf{k}} \frac{V x_0 - I\phi_0}{2E_{\mathbf{k}}^F} \tanh\left(\frac{\beta}{2} E_{\mathbf{k}}\right),$$
$$x_0 = \frac{1}{N} \sum_{\mathbf{k}} \frac{V x_0 - I\phi_0}{2E_{\mathbf{k}}} \tanh\left(\frac{\beta}{2} E_{\mathbf{k}}\right), \tag{A27}$$

which recovers the result from the coherent-state path integral, i.e., Eqs. (29) in the limit of small ϕ_0, in which the term $g N \hbar \beta |\phi_0|^2 \phi_0$ can be neglected (i.e., on the phase boundary).

Moreover, it is also worth adding that the above derivation of equations for order parameters x_0 and ϕ_0 [i.e., Eq. (A27)] can also be handled by using an explicit form of the thermodynamic potential,

$$\Omega = \Omega_F + \Omega_{FB} + \Omega_B, \tag{A28}$$

where

$$\Omega_F/N = \frac{1}{N} \sum_{\mathbf{k}} (\xi_{\mathbf{k}} - E_{\mathbf{k}}) + V|x_0|^2 - \frac{2}{\beta N} \sum_{\mathbf{k}} \ln(1 + e^{-\beta E_{\mathbf{k}}}), \tag{A29}$$

$$\Omega_{FB}/N = -I(\bar{x}_0 \phi_0 + x_0 \bar{\phi}_0), \tag{A30}$$

Ω_B/N
$$= -\frac{1}{\beta} \ln \mathrm{Tr} e^{-\beta[zJ|\phi_0|^2 + (Ix_0 - zJ\phi_0)b_i^{\dagger} + (I\bar{x}_0 - zJ\bar{\phi}_0)b_i - \mu^* b_i^{\dagger} b_i + U b_i^{\dagger} b_i^{\dagger} b_i b_i]}. \tag{A31}$$

Then extremizing Ω in terms of $\bar{x}_0$ and $\bar{\phi}_0$ yields general mean-field equations for the order parameters

$$x_0 = \frac{1}{N} \sum_{\mathbf{k}} \frac{V x_0 - I\phi_0}{2E_{\mathbf{k}}} \tanh\left(\frac{\beta}{2} E_{\mathbf{k}}\right), \tag{A32}$$

$$\phi_0 = \frac{1}{N} \sum_i \langle b_i \rangle_B, \tag{A33}$$

where $\langle \cdot \rangle_B = \mathrm{Tr} \ldots e^{-\beta H_{\mathrm{eff}}^{\mathrm{bos}}}/Z$, $Z = \mathrm{Tr} e^{-\beta H_{\mathrm{eff}}^{\mathrm{bos}}}$, and should be compared to Eqs. (A27) or (29), which were evolved close to the phase boundary. Moreover, from Eqs. (A28)–(A31), it is easy to notice that the thermodynamic potential Ω consists of a standard BCS-like part Ω_{fer}, BHM-like part Ω_{bos}, and part $\Omega_{\mathrm{fer-bos}}$, which is proportional to Feshbach interaction energy I. Equations (A28)–(A33) also make a clear framework for further analysis of the thermodynamic properties of the BFHM. As an example, the free energy F is now simply given by $F/N = \Omega/N + \mu n$ in which

$$n = -\frac{1}{N} \frac{\partial \Omega}{\partial \mu} = n_F + 2n_B, \tag{A34}$$

$$n_F = \frac{1}{N} \sum_{\mathbf{k}} \left[1 - \frac{\xi_{\mathbf{k}}}{E_{\mathbf{k}}} \tanh\left(\frac{\beta}{2} E_{\mathbf{k}}\right)\right], \tag{A35}$$

$$n_B = \frac{1}{N} \sum_i \langle b_i^{\dagger} b_i \rangle_B. \tag{A36}$$

These mean-field results should also be compared with Eqs. (37)–(39) in which the zeroth-order approximation was imposed on the statistical sum. Interestingly, the form of Ω_B and ϕ_0 given in Eqs. (A31) and (A33) can be calculated exactly for limiting cases of hard-core bosonic interaction ($U \to \infty$) and for the case where U vanishes ($U = 0$). For example, within the hard-core limit, the on-site bosonic density basis is restricted to two occupation numbers (i.e., to 0 or 1 boson per site) and then one gets $\Omega_{bos}/N = zJ|\phi_0|^2 - \mu^* - \ln[2\cosh(\beta E_g)]/\beta$, where $E_g = \sqrt{(\mu^*)^2 + |Ix_0 - zJ\phi_0|^2}$, and for order parameter ϕ_0, one finds $\phi_0 = -(Ix_0 - zJ\phi_0)\tanh(\beta E_g)/2E_g$ [2].

At the end of this section, we would like to also add that going beyond the critical line toward the SF phase, it is worth mentioning that the functional integral approach presented in Sec. II and the operator approach discussed here give different descriptions. Indeed, evaluation of the expansion in Eq. (A26)

to the third order in the ϕ_0 and x_0 amplitudes generates coefficients with a four-point local bosonic correlation function, denoted by $G_i^{2,c}(\tau_1', \tau_2', \tau_1, \tau_p)$ [see Eq. (15)], while the path-integral method gives $\Gamma_i^{2,c}(\tau, \tau', \tau'', \tau''')$ [see Eq. (24)]. This higher-order term in the path-integral formulation is denoted by g in Eq. (29), which is proportional to $\Gamma_i^{2,c}$ in

the static limit. Therefore, on the grounds of the previous considerations within the BHM in Ref. [28], we would like to point out that our path-integral formulation should be more relevant than the operator ones because its gives a better description of the Gaussian fluctuation in the BHM limit with the SF phase.

[1] J. Ranninger and S. Robaszkiewicz, Physica B+C **135**, 468 (1985).

[2] S. Robaszkiewicz, R. Micnas, and J. Ranninger, Phys. Rev. B **36**, 180 (1987).

[3] R. Micnas, J. Ranninger, and S. Robaszkiewicz, Rev. Mod. Phys. **62**, 113 (1990).

[4] R. Friedberg and T. D. Lee, Phys. Rev. B **40**, 6745 (1989).

[5] R. Friedberg, T. D. Lee, and H. C. Ren, Phys. Rev. B **42**, 4122 (1990).

[6] V. B. Geshkenbein, L. B. Ioffe, and A. I. Larkin, Phys. Rev. B **55**, 3173 (1997).

[7] A. H. Castro Neto, Phys. Rev. B **64**, 104509 (2001).

[8] T. Domański and J. Ranninger, Phys. Rev. B **63**, 134505 (2001).

[9] R. Micnas, S. Robaszkiewicz, and A. Bussmann-Holder, Phys. Rev. B **66**, 104516 (2002).

[10] T. Domański, M. M. Maśka, and M. Mierzejewski, Phys. Rev. B **67**, 134507 (2003).

[11] T. Domański and J. Ranninger, Phys. Rev. B **70**, 184503 (2004).

[12] R. Micnas, S. Robaszkiewicz, and A. Bussmann-Holder, in *Superconductivity in Complex Systems. Structure and Bonding*, edited by K. A. Müller and A. Bussmann-Holder (Springer, Berlin, Heidelberg, 2005), Vol. 114, p. 13.

[13] W.-F. Tsai and S. A. Kivelson, Phys. Rev. B **73**, 214510 (2006).

[14] K.-Y. Yang, E. Kozik, X. Wang, and M. Troyer, Phys. Rev. B **83**, 214516 (2011).

[15] R. Micnas, Philos. Mag. **95**, 622 (2015).

[16] K. V. Krutitsky, Phys. Rep. **607**, 1 (2016).

[17] I. Bloch, J. Dalibard, and W. Zwerger, Rev. Mod. Phys. **80**, 885 (2008).

[18] I. Bloch, J. Dalibard, and S. Nascimbène, Nat. Phys. **8**, 267 (2012).

[19] M. Holland, S. J. J. M. F. Kokkelmans, M. L. Chiofalo, and R. Walser, Phys. Rev. Lett. **87**, 120406 (2001).

[20] Q. Chen, J. Stajic, S. Tan, and K. Levin, Phys. Rep. **412**, 1 (2005).

[21] Y. Ohashi and A. Griffin, Phys. Rev. Lett. **89**, 130402 (2002).

[22] M. Lewenstein, A. Sanpera, and V. Ahufinger, *Ultracold Atoms in Optical Lattices* (Oxford University Press, Oxford, 2012).

[23] R. Micnas, Phys. Rev. B **76**, 184507 (2007).

[24] M. Cuoco and J. Ranninger, Phys. Rev. B **74**, 094511 (2006).

[25] J. Ranninger and L. Tripodi, Phys. Rev. B **67**, 174521 (2003).

[26] F. Zhou and C. Wu, New J. Phys. **8**, 166 (2006).

[27] A. Altland and B. D. Simons, *Condensed Matter Field Theory* (Cambridge University Press, Cambridge, 2010).

[28] K. Sengupta and N. Dupuis, Phys. Rev. A **71**, 033629 (2005).

[29] Y. Ohashi and A. Griffin, Phys. Rev. A **67**, 033603 (2003).

[30] Y. Ohashi and A. Griffin, Phys. Rev. A **67**, 063612 (2003).

[31] J. Ranninger and J. M. Robin, Phys. Rev. B **53**, R11961 (1996).

[32] J. Ranninger and J.-M. Robin, Phys. Rev. B **56**, 8330 (1997).

[33] N. Dupuis, Nucl. Phys. B **618**, 617 (2001).

[34] M. P. Kennett and D. Dalidovich, Phys. Rev. A **84**, 033620 (2011).

[35] M. R. C. Fitzpatrick and M. P. Kennett, arXiv:1801.01776.

[36] K. Sheshadri, H. R. Krishnamurthy, R. Pandit, and T. V. Ramakrishnan, Europhys. Lett. **22**, 257 (1993).

[37] S. Trotzky, L. Pollet, F. Gerbier, U. Schnorrberger, I. Bloch, N. V. Prokof'ev, B. Svistunov, and M. Troyer, Nat. Phys. **6**, 998 (2010).

[38] A. S. Sajna, T. P. Polak, R. Micnas, and P. Rożek, Phys. Rev. A **92**, 013602 (2015).

[39] F. Gerbier, Phys. Rev. Lett. **99**, 120405 (2007).

[40] R. Micnas, S. Robaszkiewicz, and A. Bussmann-Holder, Physica C: Supercond. **387**, 58 (2003).

[41] C. J. Kennedy, W. C. Burton, W. C. Chung, and W. Ketterle, Nat. Phys. **11**, 859 (2015).

[42] F. Gerbier, S. Trotzky, S. Fölling, U. Schnorrberger, J. Thompson, A. Widera, I. Bloch, L. Pollet, M. Troyer, B. Capogrosso-Sansone *et al.*, Phys. Rev. Lett. **101**, 155303 (2008).

[43] I. B. Spielman, W. D. Phillips, and J. V. Porto, Phys. Rev. Lett. **98**, 080404 (2007).

[44] F. Gerbier, A. Widera, S. Fölling, O. Mandel, T. Gericke, and I. Bloch, Phys. Rev. Lett. **95**, 050404 (2005).

[45] M. Greiner, O. Mandel, T. Esslinger, T. W. Hänsch, and I. Bloch, Nature (London) **415**, 39 (2002).

[46] T. Rom, T. Best, D. van Oosten, U. Schneider, S. Fölling, B. Paredes, and I. Bloch, Nature (London) **444**, 733 (2006).

[47] J. K. Chin, D. E. Miller, Y. Liu, C. Stan, W. Setiawan, C. Sanner, K. Xu, and W. Ketterle, Nature (London) **443**, 961 (2006).

[48] T. Best, S. Will, U. Schneider, L. Hackermüller, D. van Oosten, I. Bloch, and D.-S. Lühmann, Phys. Rev. Lett. **102**, 030408 (2009).

[49] K. Günter, T. Stöferle, H. Moritz, M. Köhl, and T. Esslinger, Phys. Rev. Lett. **96**, 180402 (2006).